

Submitted to the Editor of ApJ Letter on July 16, 2001

## **Detection of X-ray Emission from the Arches Cluster Near the Galactic Center**

F. Yusef-Zadeh

Department of Physics and Astronomy, Northwestern University, Evanston, IL 60208  
(zadeh@northwestern.edu)

C. Law

Harvard-Smithsonian Center for Astrophysics, Cambridge, MA. 02138  
(claw@head-cfa.harvard.edu)

M. Wardle

School of Physics, University of Sydney, NSW 2006, Australia  
(wardle@physics.usyd.edu.au)

Q. D. Wang

University of Massachusetts, Amherst, MA 01003-4517 (wqd@hnr.astro.umass.edu)

A. Fruscione

Harvard-Smithsonian Center for Astrophysics, Cambridge, MA. 02138  
(antonell@head-cfa.harvard.edu)

C.C. Lang

University of Massachusetts, Amherst, MA 01003-4517 (clang@ocotillo.astro.umass.edu)

A. Cotera

University of Arizona, Steward Observatory, Tucson, AZ 85721 (cotera@as.arizona.edu)

Received 00 2001;    accepted 00 2001

## ABSTRACT

The Arches cluster is an extraordinarily compact massive star cluster with a core radius of about  $10''$  ( $\sim 0.4$  pc) and consisting of more than 150 O star candidates with initial stellar masses greater than  $20 M_{\odot}$  near G0.12-0.02. X-ray observations of the radio Arc near the Galactic center at  $l \sim 0.2^{\circ}$  which contains the Arches cluster have been carried out with the Advanced CCD Imaging Spectrometer (ACIS) on board Chandra X-ray Observatory. We report the detection of two X-ray sources from the Arches cluster embedded within a bath of diffuse X-ray emission extending beyond the edge of the cluster to at least  $90'' \times 60''$  ( $3.6 \text{ pc} \times 2.4 \text{ pc}$ ). The brightest component of the X-ray emission coincides with the core of the cluster and can be fitted with two-temperature thermal spectrum with a soft and hard component of 0.8 and 6.4 keV, respectively. The core of the cluster coincides with several ionized stellar wind sources that have previously been detected at radio wavelengths, suggesting that the X-ray emission from the core arises from stellar wind sources. The diffuse emission beyond the boundary of the cluster is discussed in the context of combined shocked stellar winds escaping from the cluster. We argue that the expelled gas from young clusters such as the Arches cluster may be responsible for the hot and extended X-ray emitting gas detected throughout the inner degree of the Galactic center.

*Subject headings:* galaxies: ISM—Galaxy: center —X-rays: ISM – stars: mass loss –stars: winds

## 1. Introduction

Near-IR observations of the Galactic center region have recently identified two clusters of young and massive stars embedded within the radio Arc at galactic longitude  $l \sim 0.2^\circ$  lying within 25 pc in projection from the Galactic center at a distance of 8.5 kpc. (Nagata *et al.* 1995; Cotera *et al.* 1996; Serabyn, Shupe, & Figer 1998; Figer *et al.* 1999). The two stellar clusters, which are responsible for ionizing the thermal components of the radio Arc, show similar characteristics to the IRS 16 cluster at the Galactic center (Simons, Hodapp & Becklin 1990; Allen *et al.* 1990, Krabbe *et al.* 1991).

Zwart *et al.* (2001) have recently predicted that the Galactic center region may contain a large number of young and massive clusters similar to the Arches, Quintuplet and IRS 16 clusters. Understanding their nature is an important step towards determining the rate of massive star formation in this unique region of the Galaxy.

The Arches cluster has an angular size of  $\sim 15''$  with a peak density of  $3 \times 10^5 M_\odot \text{pc}^{-3}$  in the inner  $9''$  (0.36 pc) (Figer *et al.* 1999). This cluster is one of the densest known young clusters in the local group of galaxies with densities similar to R136, the central cluster of 30 Dor in the Large Magellanic Cloud and NGC 3603; the Trapezium cluster in Orion has a density of  $7 \times 10^4 M_\odot \text{pc}^{-3}$  (Brandl *et al.* 1996; Wang 1999; McCaughrean & Stauffer 1994; Brandl *et al.* 1999). The Arches cluster has an estimated age of 1–3 Myr and shows a flat mass function as compared to other young clusters (Figer *et al.* 1999). The Quintuplet cluster adjacent to the Sickle is less compact, and is 3–5 Myr old (Figer, McLean and Morris 1999). Radio continuum emission from individual stars in both clusters has recently been detected (Lang *et al.* 1999; 2001). Radio spectral index and near-IR spectral type of several stars in the Arches cluster are consistent with ionized stellar winds arising from mass-losing WN and/or Of stars with mass-loss rates  $\approx (1 - 20) \times 10^{-5} M_\odot \text{yr}^{-1}$  and lower limits to their winds' terminal velocities range between 800 and 1200  $\text{kms}^{-1}$  (Cotera *et al.* 1996).

## 2. Observations

The X-ray imaging of the inner degree of the Galactic center region dates back to Einstein and SL2-XRT, ROSAT, ASCA observations where a number of point sources and diffuse emission were detected (Watson *et al.* 1981; Skinner *et al.* 1987; Predehl and Trümper 1994; Koyama *et al.* 1996). The Advanced CCD Imaging Spectrometer (ACIS) on board the Chandra X-Ray Observatory (Weisskopf *et al.* 1996; Garmire *et al.* 2000) was used to observe the radio Arc on July 7, 2000 for a total observing time 51 kseconds. The observation was made in the ACIS-I configuration, with a nominal aim-point toward the linear filaments of the radio Arc (epoch 2000)  $\alpha = 17^h46^m22^s, \delta = -28^\circ51'36.4''$ . In total, six of the ACIS CCDs were readout: the imaging array, I0-I3, and two of the spectroscopy array, S2 and S3. Only the data from the imaging array, particularly the I1 chip, will be presented here. The data were processed using the Chandra X-ray Center’s CIAO software package (Noble *et al.* 2000). The images are effectively flat-fielded: instrument response and effective area are divided out in the form of an “exposure map”.

## 3. Results

Figure 1a shows a flux image of X-ray emission detected in ACIS’s I<sub>0</sub> to I<sub>3</sub> detectors with prominent sources labeled. Two sources located to the northwest of the image coincide with the Arches cluster. These sources avoid the strong diffuse X-ray emission arising from the Galactic plane of the Galactic center region. We note a prominent diffuse structure on a scale of about  $2' \times 2'$  centered near (epoch 2000)  $\alpha = 17^h46^m18^s, \delta = -28^\circ54'$ . This diffuse feature shows two linear X-ray structures. Using the Very Large Array of the National

Radio Astronomy Observatory<sup>1</sup> a  $\lambda 20\text{cm}$  continuum image with a resolution of  $10.7'' \times 10''$  (Yusef-Zadeh, Morris and Chance 1984) is compared with identical region to that of Figure 1a and is displayed in Figure 1b where Sgr A complex is located to the SW corner. The northern X-ray filament appears to be situated at the inner boundary of a number of nonthermal radio filaments running perpendicular to the Galactic plane.

Figure 2a shows contours of adaptively smoothed X-ray emission in a smaller region around the Arches cluster, with five components being identified and labeled as A1–A5. The crosses show the positions of the compact radio sources which are due to free-free emission from ionized stellar winds (Lang *et al.* 2001). The brightest component of X-ray emission (A1) is centered on the SW corner of the densest part of the core of the Arches cluster where the largest concentration of ionized stellar wind radio sources has been detected. The near-IR counterparts to radio sources are identified as either WN or Of spectral types (Nagata *et al.* 1995; Cotera *et al.* 1996).

A close-up view is displayed in Figure 2b where the X-ray contours have been superimposed on a grayscale image of the stellar sources obtained with NICMOS on the HST (Figer *et al.* 1999). The brightest *radio* source, an Of/WN9 star (star no. 8 in Nagata *et al.* 1995 and Cotera *et al.* 1996) estimated to have a mass-loss rate of  $1.7 \times 10^{-4} M_{\odot} \text{yr}^{-1}$  (Lang *et al.* 2001), lies very close to the geometric center of A1. These facts strongly suggest that A1 is associated with the core of the Arches cluster. The second X-ray component (A2) lies about  $10''$  NW of A1 and appears to be located outside the core of the cluster but still close to the outer boundary. No radio emitting stellar sources have been detected toward A2. The peak of A2 coincides within  $1''$  with a star classified an emission line star, WN7, WN8 or Of4 (Cotera *et al.* 1996, Blum *et al.* 2001). The largest scale

---

<sup>1</sup>The National Radio Astronomy Observatory is a facility of the National Science Foundation, operated under a cooperative agreement by Associated Universities, Inc.

component of X-ray emission in Figure 2a is a diffuse ovoid feature (A3) which envelops both A1 and A2, and is elongated at a position angle of  $102^\circ$  E of N from the Galactic plane. With dimensions of approximately  $90'' \times 60''$  ( $3.6 \times 2.4$  pc), A3 extends well beyond the edge of the cluster, which is  $\lesssim 15''$  in diameter. Two point-like (A4 and A5) lie to the east and west of the cluster at (J2000)  $\alpha = 17^h45^m55.84^s$ ,  $\delta = -28^\circ49'15.1''$  and (J2000)  $\alpha = 17^h45^m45.25^s$ ,  $\delta = -28^\circ49'26.1''$ . The nature of A4 and A5 as well as a number of extended and sharp features observed in high-resolution X-ray images will be discussed elsewhere.

Figures 3a,b and c show the observed and modeled spectra toward the A1, A2 and A3 components. The spectra of A1 and A2 were fitted with a MEKAL model (Mewe *et al.* 1985) of a two-temperature thermal plasma. The two sources were permitted to have different temperatures and volume emission measures, but the abundances and absorbing column densities were constrained to be identical. Table 1 shows the parameters of the A1 and A2 model fits and one  $\sigma$  uncertainty and the associated 68% confidence level. The spectra are best fitted by thermal bremsstrahlung with two temperatures at 0.8 and 6.4 keV for A1 and 0.9 and 5.8 keV for A2. The respective X-ray luminosities ( $L_X$ ) of A1 and A2 integrated between 0.2 and 10 keV, give  $3.3$  and  $0.8 \times 10^{35}$  ergs s $^{-1}$  with a total  $L_X \sim 4.1 \times 10^{35}$  ergs s $^{-1}$ .

The heavy element abundances in the X-ray emitting plasma range from 1.6 to 3.8 solar, similar to other determinations in the Galactic center region (Maeda *et al.* 2001; Baganoff *et al.* 2001). The absorption column of  $12.4_{-2}^{+2.9} \times 10^{22}$  H cm $^{-2}$  toward the Arches cluster corresponds to a visual extinction of  $A_V \sim 69_{-11}^{+16}$  mag, similar to that inferred from Chandra and ROSAT observations toward Sgr A East and Sgr A\* at the Galactic center (Maeda *et al.* 2001; Baganoff *et al.* 2001; Predehl and Trümper 1994). There seems to be a systematic discrepancy between X-ray estimates of  $A_V$  and the value  $\sim 30$  inferred

from near-IR observations toward the Arches cluster and the Galactic center (Serabyn *et al.* 1998; Rieke and Lebofski 1985). Note that the fits to the spectra are poorer (reduced chi-square  $\sim 1.5$ ) when  $N_H$  is set to  $6 \times 10^{22} \text{ H cm}^{-2}$ , corresponding to  $A_V = 30 \text{ mag}$ .

After the A1 and A2 components are subtracted the spectrum of A3 is fit by a single thermal bremsstrahlung of temperature  $5.7_{4.4}^{13.5} \text{ keV}$ , an absorbing column of  $10.1_{7.9}^{13.5} \times 10^{22} \text{ H cm}^{-2}$  and an additional Gaussian contributed by fluorescent Fe K/ $\alpha$  6.4 keV line emission. The upper bound to the temperature is unconstrained due to the low number of counts at high energies and the restricted energy band, although the estimated temperatures of A1, A2 and A3 are the same within errors. The total X-ray luminosity of A3 between 0.5 and 10 keV excluding the 6.4 keV line is  $L_X \approx 1.6 \times 10^{34} \text{ ergs s}^{-1}$ .

#### 4. Discussion

The Arches cluster was positioned on the I1 chip, about  $7'$  away from the telescope's aimpoint. The shape and the size of the PSF at this location is fitted by an elliptical Gaussian with  $\text{FWHM} = 4.4'' \times 2.2''$  and  $\text{PA} = 83^\circ$ . Sources A1 and A2 are fitted by elliptical Gaussians with  $\text{FWHM} 8.0'' \times 7.1''$  ( $\text{PA} = 96^\circ$ ) and  $7.9'' \times 5.1''$  ( $\text{PA} = 90^\circ$ ), respectively, indicating that they are partially resolved. Further observations are needed to confirm the true extent of A1 and A2.

The resulting distortion of A1 and A2 caused by the point spread function (PSF) means that the present observations cannot distinguish between compact emission associated with the collisions between the ionized winds from early-type stars paired in binary systems and more extended emission arising as a result of the interaction between winds from individual stars within the cluster. Figure 2b suggests an association of the A1 component with the known stellar wind sources in the Arches cluster, and of A2 with the bright stellar source

located at (J2000)  $\alpha = 17^h45^m50.27^s$ ,  $\delta = -28^\circ49'11.64''$  which is identified as either a WN8 or an Of4 star (star number 1 in Cotera *et al.* 1996). The X-ray emission from the collision of winds between early-type stars and early-type companions can account for the luminosity and the temperature of A1 and A2 (Stevens *et al.* 1992). The X-ray emission from the cluster R136 is believed to be powered by a dozen colliding wind X-ray binaries. The brightest binary system (CX5 in Zwart *et al.* 2001) has X-ray luminosity of  $2 \times 10^{35}$  ergs  $s^{-1}$  and a fitted temperature of 2.3 keV (Zwart, Walter and Lewin 2001).

The A3 component is unlikely to arise from individual stellar sources or binary systems associated with the cluster as it extends far beyond the cluster boundary. A more likely source is the shock-heated gas created by the collision of individual  $\sim 1000$  km/s stellar winds in the dense cluster environment (Ozernoy, Genzel and Usov 1997; Cantó *et al.* 2000). This gas is far too hot to be bound to the cluster, escaping as a supersonic wind provided the external pressure of the medium is not too high. The electron density and mass of A3 implied by our observations are  $1.9 \text{ cm}^{-3}$  and  $0.4 M_\odot$ , respectively. Using the total mass loss rate  $\sim 4 \times 10^{-4} M_\odot \text{ yr}^{-1}$  estimated from the radio continuum sources detected in the cluster (Lang *et al.* 2001), we estimate that the residence time of the gas in the A3 component is about  $10^3$  years. As predicted by the model (Cantó *et al.* 2000), the required flow velocity of the wind, about  $1200 \text{ km s}^{-1}$ , is comparable to the stellar wind speeds determined from the spectra of cluster members (Cotera *et al.* 1996). The elongation of the X-ray emission from A3 perpendicular to the Galactic plane may be an indication that the cluster wind flow is confined more by the ISM in the galactic plane than normal to it.

The X-ray emission from the wind is dominated by the portion within the cluster boundary, thus either or both of the A1 and A2 components may be produced by the wind. The total X-ray flux between 0.2 and 10 keV from A1, A2 and A3 is  $\sim 5 \times 10^{35} \text{ erg s}^{-1}$  which is close to the X-ray luminosity of  $6 \times 10^{35} \text{ ergs s}^{-1}$ , predicted by Cantó *et al.* (2000).



Their temperature estimate also agrees with the high temperature component of A1 (if a mean molecular weight of  $2m_H$  is assumed instead of  $2/3 m_H$ ).

Where does the hot gas go after it escapes from the cluster? Theoretical studies predict that at any one time the inner 200 pc of the Galaxy may harbor 50 clusters like the Arches with lifetimes of roughly 70 Myr (Zwart *et al.* 2001). It is possible that the gas expelled from the Arches clusters and others like it contributes to the extremely hot diffuse gas found in the inner degree of the Galactic center. The electron temperature of the hot gas is about 10 keV, with an electron density of  $0.3\text{--}0.4 \text{ cm}^{-3}$  and a total mass of about  $2\text{--}4 \times 10^3 M_\odot$  (e.g. Yamauchi *et al.* 1990; Koyama *et al.* 1996). The hot plasma at this temperature can not be confined by the gravitational potential in the Galactic center region, and if unhindered escapes the region on a time scale of  $10^5$  years. The required replenishment rate is therefore  $\sim 3 \times 10^{-2} M_\odot \text{ yr}^{-1}$ , which could be supplied by the gas lost from 50 clusters like the Arches cluster in the inner 200 pc. However, if the strength of the magnetic field in the inner degree is about one milliGauss, as a number of studies indicate (e.g. Yusef-Zadeh, Morris and Chance 1984; Yusef-Zadeh and Morris 1987; Lang, Morris and Echevarria 1999), then the magnetic pressure is strong enough to confine much of the hot plasma (Koyama *et al.* 1996; Yusef-Zadeh *et al.* 1997). Under this assumption, the gas must be replenished on the cooling time of  $\sim 10^8$  years, and the required input rate is 1000 times less. The confined gas can be accounted for if at any given time there is a single cluster similar to the Arches cluster within the inner degree of the Galactic center.

Searches for extended X-ray emission may prove useful in identifying young clusters near the Galactic Center. It would be worthwhile to look for X-ray emission from young cluster candidates (e.g. Dutra and Bica 2000).

Table 1. Best-fit Parameters to the Components of the Arches Cluster

Source	Parameter	Best fit (error bars)
A1	kT(1)[keV]	6.4 (-1.5, +2.8)
"	normalization	$3.6 \times 10^{-4}$ ( $-1.8 \times 10^{-4}$ , $+2.2 \times 10^{-4}$ )
"	kT(2)[keV]	0.8 (-0.2, +0.2)
"	normalization	$8.3 \times 10^{-3}$ ( $-5.5 \times 10^{-3}$ , $+2.3 \times 10^{-2}$ )
"	chi-squared per degree of freedom	0.98
A2	kT(1)[keV]	1.0 (-0.4, +0.6)
"	normalization	$2.0 \times 10^{-3}$ ( $-1.3 \times 10^{-3}$ , $+1.0 \times 10^{-2}$ )
"	kT(2)[keV]	5.8 (-2.3, +4.7)
"	normalization	$2.3 \times 10^{-4}$ ( $-1.4 \times 10^{-4}$ , $+2.1 \times 10^{-4}$ )
"	chi-squared per degree of freedom	0.97
A1, A2	$N_H [10^{22} \text{ cm}^{-2}]$	12.4 (-2.0, +2.9)
"	Si/Si $\odot$	2.9 (-1.7, +3.7)
"	S/S $\odot$	1.6 (-0.6, +1.0 )
"	Ar/Ar $\odot$	2.5 (-1.0, +1.3)
"	Ca/Ca $\odot$	3.9 (-1.4, +1.7)
"	Fe/Fe $\odot$	2.2 (-0.8, 1.7)

## REFERENCES

- Allen, D.A., Hyland, A.R. & Hillier, D.J. 1990, MNRAS, 244, 706
- Baganoff, F.K., Maeda, Y., Morris, M., Bautz, W.N., Brandt, W. *et al.* 2001, ApJ, 2001, in press
- Blum, R.D., Schaerer, D., Pasquali, A., Heydari-Malayeri, M., Conti, P.S., Schultz, W. 2001, arXiv:astro-ph/0106496
- Brandl, B. *et al.* 1996, ApJ, 466, 254
- Brandl, B., Brandner, W., Eisenhauer, F., Moffat, A. F. J., Palla, F., Zinnecker, H. 1999, A.A. 352, L69
- Cantó, J., Raga, A.C. & Rodriguez, L.F. 2000, ApJ, 536, 896
- Cotera, A., Erickson, E., Colgan, S., Simpson, J., Allen, D. & Burton, M. 1996, ApJ, 461, 750
- Dutra, C.M. & Bica, E. 2000, A.&A. 359, L9
- Eckart, A., Genzel, R., Krabbe, A., Hofmann, R., van der Werf, P. P. & Drapatz, S. 1992, Nature, 355, 526.
- Figer, D.F., McLean, I.S. & Morris, M., 1999, ApJ, 514, 202
- Figer, D.F., Sungsoo, S.K., Morris, M., Serabyn, E., Rich, R.M., McLean, I.S. 1999, ApJ, 525, 750
- Geballe, T. R., Krisciunas, K., Bailey, J. A. & Wade, R. 1991, ApJ, 370, L73
- Koyama, K., Maeda, Y., Sonobe, T., Takeshima, T., Tanaka, Y. *et al.* 1996, PASJ, 48, 249
- Krabbe, A., Genzel, R., Drapatz, S. & Rotacijs, V. 1991, ApJ, 382, L19
- Lang, C.C., Goss, W.M. & Rodriguez, L. 2001, ApJ, 551, L143
- Lang, C., Morris, M. & Echevarria, L. 1999, ApJ, 526, 727

- Lang, C.C., Figer, D.F., Goss, W.M. & Morris, M. 1999, AJ, 118, 2327
- Noble, M.S., 2000, in ADASS IX, ASP Conference Proceedings, Vol. 216, edited by Nadine Manset, Christian Veillet, and Dennis Crabtree, 603
- Maeda, Y., Baganoff, F.K., Feigelson, M.W., Bautz, W.N., Brandt, D.N. *et al.* 2001, ApJ, in press.
- McCaughrean, M.J. & Stauffer, J.R. 1994, AJ 108, 1382
- Mewe, R., Gronesechild, E.H.B.M., & van den Oord, G.H.J. 1985, A&AS, 62, 197
- Nagata, T., et al. 1995, AJ, 109, 1676
- Ozernoy, L.M., Genzel, R. & Usov, V. 1997, MNRAS, 288, 237
- Predehl, P. and Trümper 1994, A.&A., 290, L29
- Rieke, G. H. & Lebofsky, M.J. 1985, ApJ, 288, 618
- Schulz, N.S., Canzianes, C., Huenemoerder, D., Kastner, J.H., Taylor, S.C. *et al.* 2001, ApJ, 549, 441
- Schulz, N.S., Canzianes, C., Huenemoerder, D. & Lee, J.C. 2001, 2000, ApJ, 545, L135
- Simons, D.A., Hoddapp, K.W. & Becklin, E.E. ApJ, 360, 106
- Serabyn, E., Shupe, D., & Figer, D. F. 1998, Nature, 394, 448
- Skinner, G.K., Wilmore, A.P., Eyles, C.J., Bertram, D. *et al.* 1981, Nature, 330, 544
- Stevens, I.R., Blondin, J.M. & Pollack, A.M. 1992, ApJ, 386, 265
- Wang, Q.D. 1999, ApJL, 510. 139
- Watson, M.G., Willingate, R., Grindlay, J.E. & Herts, P. 1981, ApJ, 250, 142
- Weisskopf, M.C., O'Dell, S. & van Speybroeck, L.P. 1996, Proc. SPIE, 2805, 2
- Yamauchi, S., Kawada, M., Koyama, K., Kunieda, H. & Tawara, Y. 1990, ApJ, 365, 532

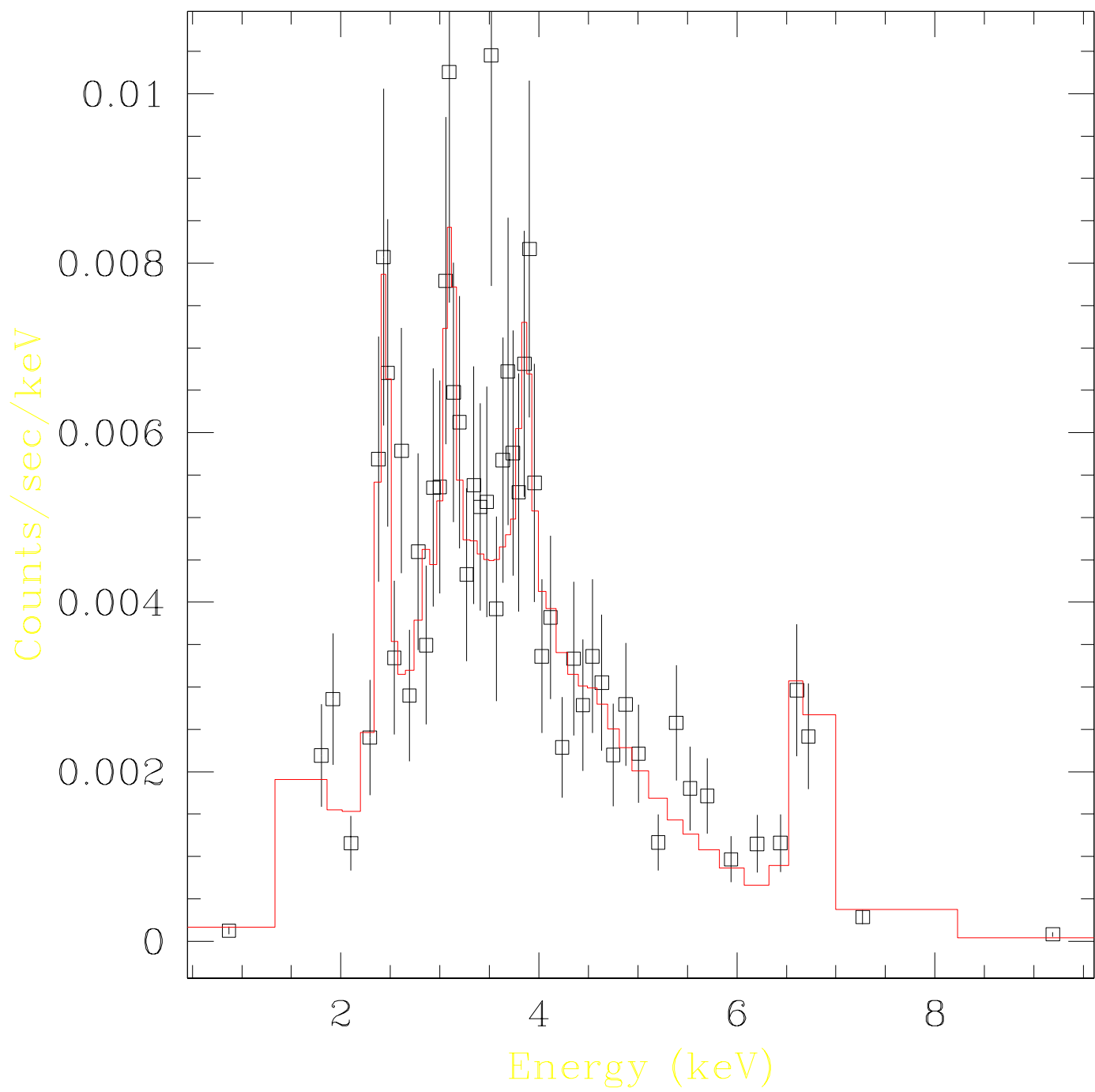
- Yusef-Zadeh, F. and Morris, M. 1987, ApJ, 320, 545
- Yusef-Zadeh, F., Morris, M. & Chance D. 1984, Nature, 310, 557
- Yusef-Zadeh, F., Purcell, W. & Gothelf, E. 1997, Proceedings of the 4th Compton Symposium, eds: D. Dermer, M.S. Strickman and J.D. Kurfess, p. 1027.
- Zwart, S.F.P., Makino, J., McMillan, W. & Hut, P. 2001, ApJ, 546, L101
- Zwart, S.F.P., Walter, D.P. & Lewin, H.G. 2001, arXiv.astro-ph/0106109.

Fig. 1.— (1a) An image of Chandra’s four ACIS-I chips for the 0.5 to 8 keV band where diffuse emission is detected throughout this region. We note two linear X-ray structures running perpendicular to the Galactic plane. A bright source to the north at the edge of the field is identified with 1E1743.1–2843 (Watson *et al.* 1981) whereas the bright feature at the bottom right corner is associated with the Sgr A complex. (1b) A radio counterpart to an identical region of (a) but at  $\lambda 20\text{cm}$  with a spatial resolution of  $10.7'' \times 10''$ . The nonthermal radio filaments are seen prominently in the direction perpendicular to the galactic plane. The northern X-ray filament is situated at the inner boundary of the nonthermal radio filaments.

Fig. 2.— Left panel (2a) shows contours of adaptively smoothed X-ray emission of five components (A1–A5) of the Arches cluster. The crosses show the positions of mass-losing stellar wind sources identified in radio wavelengths. The total X-Ray flux of A4 and A5 are  $1.4$  and  $0.18 \times 10^{-12} \text{ ergs s}^{-1} \text{ cm}^{-2}$ , respectively. Right panel (2b) shows contours of the smoothed X-ray emission from A1 and A2 with stellar radio sources as crosses and are superimposed on the near-IR stellar distribution of the Arches cluster.

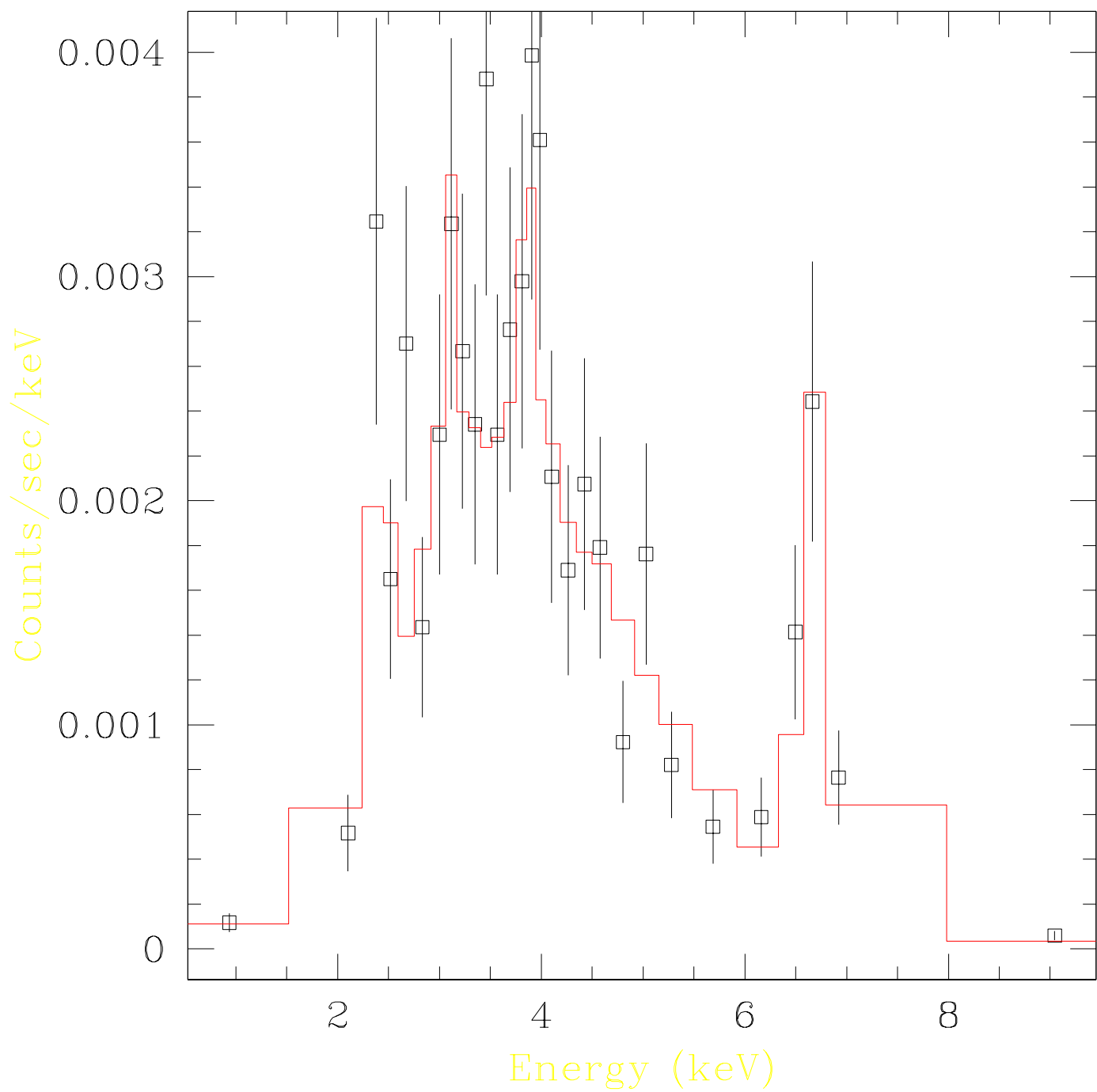
Fig. 3.— The spectra and the fits to the A1, A2 and A3 components of the Arches cluster are shown in the top left (a) and top right (b) and bottom (c) panels, respectively. The A1 and A2 fits model with an absorbed, two-temperature, thermal plasma emission model whereas the A3 fit model is an absorbed, one temperature, thermal plasma emission model with a Gaussian at 6.4 keV corresponding to the fluorescent Fe K/ $\alpha$  emission. The spectra of the A1 component of Arches cluster are extracted from an elliptical region with an extent of  $6'' \times 11''$ . The background subtracted from the is taken from the region outside of the Arches cluster, in a roughly circular region  $200''$  across. Sherpa, the fitting and modeling engine of CIAO, was used to fit the A1 and A2 spectra. We fit the spectra with "xsvmekal" (Mewe, Groneschild and ven den Oord 1985; a.k.a. "vmekal" in XSPEC), a thermal bremsstrahlung plasma model with five emission lines of varying abundance (Si, S, Ar, Ca, Fe). The thermal model was also multiplied by an absorbing column, "xswabs". For the two-temperature fits to A1 and A2, the elemental abundances and column densities of the first and second components were linked together. The thermal flux of absorbed (absorption-corrected) spectrum when integrated between 0.2 and 10 keV give  $4.8 \times 10^{-13}$  ( $3.9 \times 10^{-11}$ ) ergs  $\text{cm}^{-2} \text{s}^{-1}$  for A1 and  $2.7 \times 10^{-13}$  ( $9 \times 10^{-12}$ ) ergs  $\text{cm}^{-2} \text{s}^{-1}$  for A2 covering a region of  $5'' \times 10''$  and  $5.1 \times 10^{-13}$  ( $1.8 \times 10^{-12}$ ) ergs  $\text{cm}^{-2} \text{s}^{-1}$  for A3 covering a region of  $74'' \times 111''$  with A1 and A2 removed.

psextract\_s1.pi

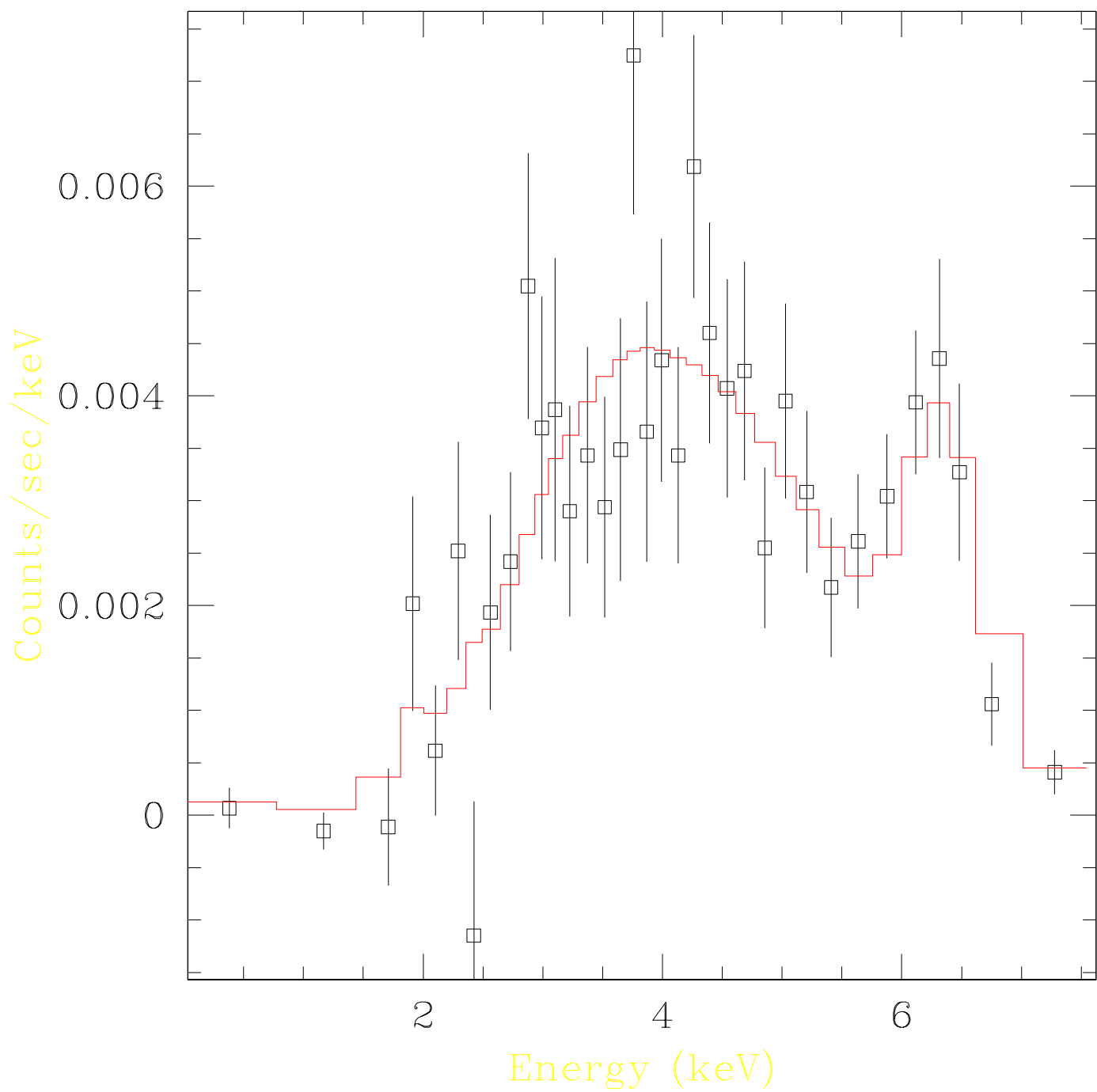




psextract\_s2.pi



psextract\_utflow.pi



This figure "gfig1a\_xray\_edit.gif" is available in "gif" format from:

<http://arXiv.org/ps/astro-ph/0108174v1>

This figure "gfig1b\_radio\_edit.gif" is available in "gif" format from:

<http://arXiv.org/ps/astro-ph/0108174v1>

This figure "fig2b\_a1a2\_edit.gif" is available in "gif" format from:

<http://arXiv.org/ps/astro-ph/0108174v1>

This figure "fig2a\_a123\_edit.gif" is available in "gif" format from:

<http://arXiv.org/ps/astro-ph/0108174v1>